Oceanic Thermal Response to Strong Atmospheric Forcing I. Characteristics of Forcing Events

RUSSELL L. ELSBERRY[1] AND NORMAN T. CAMP[2,3]

Naval Postgraduate School, Monterey, Calif. 93940

(Manuscript received 10 March 1977, in final form 21 November 1977)

ABSTRACT

Long time series of meteorological data from Ocean Weather Ships P, V and N in the North Pacific Ocean are used to test the hypothesis that significant oceanic thermal response during September to December occurs in association with limited periods of strong atmospheric forcing. The 3 h forcing is expressed according to recent mixed layer theory in terms of u_*^3, where u_* is the atmospheric friction velocity, and the upward surface heat flux. About 13% of the largest u_*^3 values contribute 50% of the total u_*^3, even though the total input is quite different at the three stations. Although the thermal forcing is less skewed, a significant fraction of this flux occurs during a relatively small fraction of the time. Synoptic time scale forcing events are defined as sustained periods of forcing exceeding the long-term mean fluxes for the corresponding period. Between 68 and 77% of the total u_*^3 occurred during the roughly one-third of the time associated with the synoptic forcing events defined in terms of u_*^3. Likewise a significant fraction of the September–December sea surface temperature change occurred during these events. Both the time and magnitude of the strong atmospheric forcing events can have a significant effect on the September–December evolution of the upper ocean thermal structure.

1. Introduction

The objective of this study is to investigate the response in the upper ocean to strong atmospheric forcing events during the fall and early winter cooling season. Simpson (1969) has suggested that significant heat, moisture and momentum fluxes are concentrated almost entirely within synoptic-scale forcing events. For example, during a three-month period of strong winter storms at Ocean Weather Ship Charlie (53°N, 35°W), 84% of the evaporation took place in only 30% of the time intervals. The momentum and sensible heat fluxes were similarly concentrated. Simpson's analysis was directed toward understanding the potential feedback role of the large heat fluxes in modifying the cyclones. The response of the upper ocean to these large heat and momentum fluxes was not considered. Long time series of meteorological observations taken at the ocean weather ship locations can be used to infer the significant characteristics of the atmospheric forcing of the ocean. Near-surface marine observations for 24, 23 and 15 years at Ocean Weather Ship *Papa* (50°N, 145°W), OWS *November* (30°N, 140°W) and OWS *Victor* (34°N, 164°E), respectively, were available from the National Weather Records Center. These locations experience a variety of storm conditions, with the effect on the air-sea interactions expected to be most pronounced at OWS V and OWS P and weakest at OWS N. Unfortunately, a similarly continuous set of oceanic observations does not exist to allow a complete specification of the oceanic response due to the passage of the storms.

In this paper some case studies with relatively frequent oceanic observations are used to demonstrate a characteristic pattern of rapid cooling and deepening of the mixed layer in conjunction with the storm passage. Then a major fraction of the atmospheric forcing is shown to be concentrated in the relatively short periods of time associated with the storms. Finally, we demonstrate that the sea surface temperature changes during strong atmospheric forcing events represent a significant fraction of the cooling of the near-surface ocean layers during the September–December period.

2. Importance of large atmospheric forcing events in the seasonal evolution of the mixed layer

We assume that the response in the mixed layer may be related to terms representing the mechanical and convective generation of turbulent kinetic energy (Camp, 1976). Values of the atmospheric friction velocity (u_*), solar radiation (Q_s) and upward surface heat flux (Q_a) were calculated from the

[1] Department of Meteorology.
[2] Department of Oceanography.
[3] Present address: Staff, COMFAIRMED, FPO New York 09521.

0022-3670/78/0206-0214$05.00

observations at the ocean weather ships using the formulas given in the Appendix. An example of distributions of the u_*^3, Q_s and Q_a values at OWS P during the cooling season is shown in Fig. 1. Both the daily mean value and the long-term mean values of u_*^3 are shown in Fig. 1D. The long-term mean increases by about a factor of 2 from September to December. As expected, the daily values have a large variation about this mean. As shown in Fig. 1C, there is also a synoptic-period variability in the Q_s and Q_a. Variations in Q_s tend to dampen as the available insolation decreases toward the winter solstice. Hence much of the net upward heat flux variability is due to Q_a. One may note that the heat flux peaks do not necessarily coincide with the u_*^3 peaks. Most of the variability in the atmospheric forcing in terms of these u_*^3 and net heat fluxes may be associated with the passage of extratropical cyclones. The purpose of this analysis is to demonstrate that significant oceanic thermal response occurs in association with the periods of strong forcing.

The response, in terms of sea surface temperature and mixed-layer depth, to this forcing is shown in Fig. 1A and 1B. At the beginning of this season the upper ocean was about 2°C warmer and the mixed layer was about 10 m shallower than the long-term means. However, these conditions were reversed by the rapid cooling and deepening following 15 October. A significant fraction of the seasonal cooling thus occurred during this relatively short period of strong atmospheric forcing. Examination of the mixed-layer depth (Fig. 1B) reveals a charac-

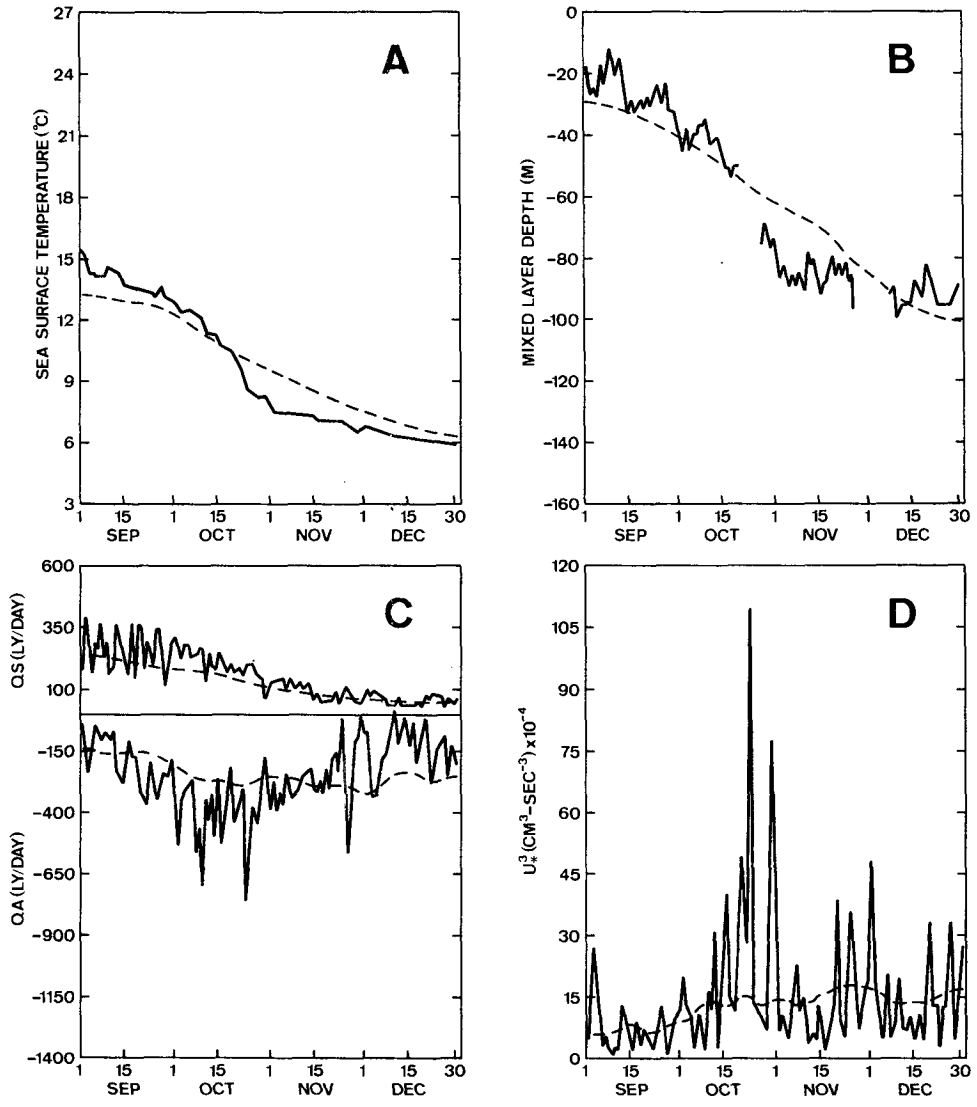

FIG. 1. Daily-averaged values of (A) sea-surface temperature, (B) mixed layer depth, (C) insolation (Q_s) and surface heat flux plus back radiation (Q_a), and (D) u_*^3 at OWS P during the 1963 season. Dashed lines represent the long-term mean (24 year) values.

teristic sawtooth pattern of rapid deepening during a period of strong forcing, but little deepening, or even layer retreat, between forcing events. The rapid deepening period corresponds to that with the largest rate of cooling. The detailed time evolution of the mixed-layer depth was not always available during strong forcing events if, as in Fig. 1B, bathythermographs were not taken. Nevertheless, one can clearly infer the association between the oceanic response and the strong atmospheric forcing. It should be emphasized that the effect of the strong forcing events depends on the initial ocean thermal structure. The large response in the 15 October case was due to the relatively warm and shallow mixed layer. Later in the season the mixed-layer depth is larger, and the amount of deepening and cooling of the layer is diminished, even with stronger forcing events. An additional impediment to further deepening of the layer at OWS P is the presence of the permanent halocline near 100 m. It is thus suggested that the timing of the strong forcing events is important with the strongest oceanic responses being produced early in the cooling season when a warm and shallow mixed layer exists.

An example illustrating the effect of the absence of forcing events at OWS P is shown in Fig. 2. During the early season the mixed layer was about 1°C cooler and nearly 20 m deeper than the long-term mean values. During a period from 15 September to 20 October u_*^3 (Fig. 2D) was less than the long-term mean, indicating a small mechanical production of turbulent kinetic energy. During most of this period the upward heat flux (Q_a) was also less than the long-term mean. Because less turbulent

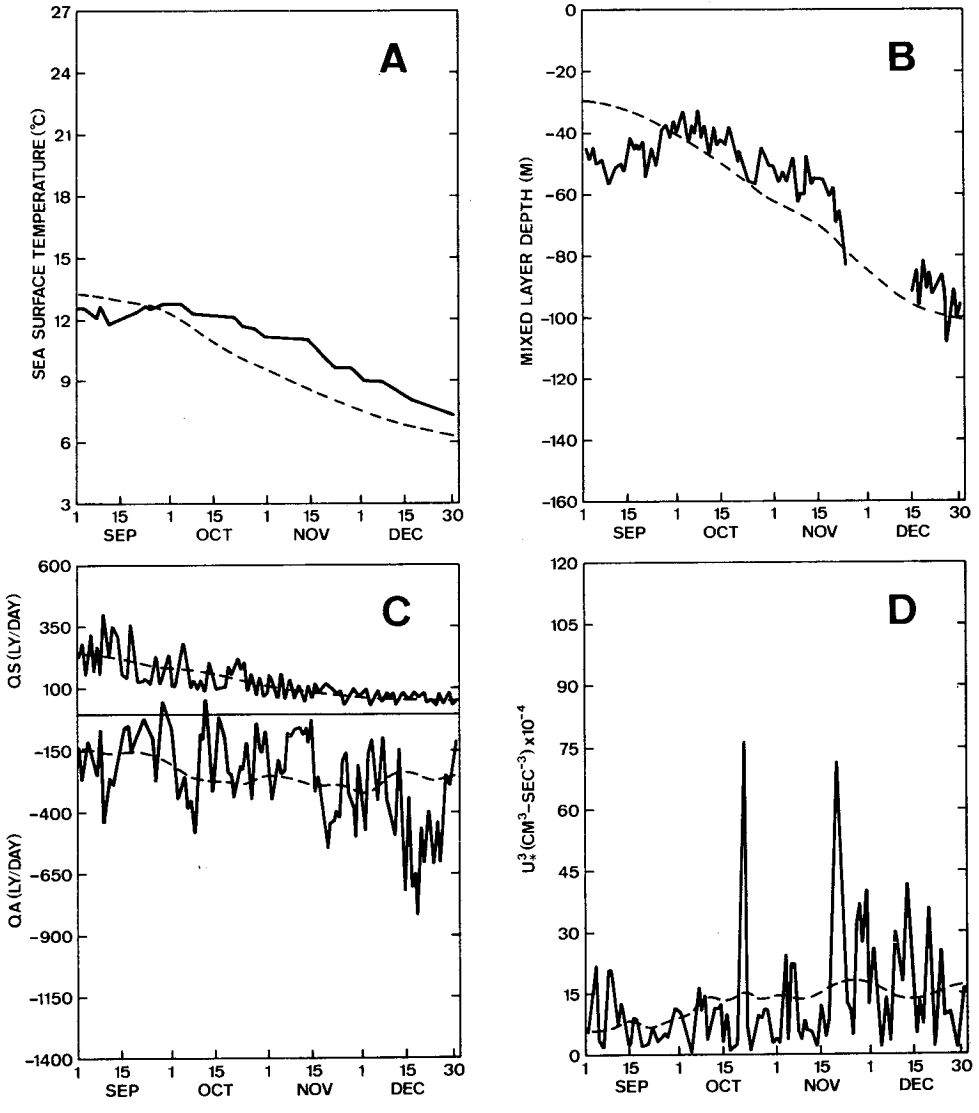

FIG. 2. As in Fig. 1 except for 1959.

kinetic energy was available for mixing during this period of net heating, the layer shallowed and warmed to a value greater than the long-term mean. The short-duration, wind-forcing event on 20 October produced some deepening and cooling, but this was followed by nearly a month of relatively weak forcing. Preceding the resumption of strong forcing on 17 November, the mixed layer was more than 2°C warmer and 15 m shallower than the long-term mean. The rate of cooling associated with the subsequent forcing is less than in the previous example because of the smaller magnitude of the forcing and the greater layer depth over which the effect is distributed.

The data in these examples tend to support the hypothesis that significant oceanic thermal response occurs in association with limited periods of strong atmospheric forcing. Unfortunately, the oceanic data were not collected as frequently as the meteorological data at the ocean weather ships. Consequently we adopt an indirect approach and calculate the atmospheric forcing over long periods and infer the oceanic response only in terms of the sea surface temperature changes. In particular, we ask the questions . . . how frequently do such strong atmospheric forcing events occur? and do they play a significant role in the cooling of the upper ocean during the September to December period?

3. Characteristics of the three-hourly atmospheric forcing

Histograms of the friction velocity and of the terms related to the mechanical (u_*^3) and convective (upward surface heat flux Q_a) generation of turbulent kinetic energy are shown in Figs. 3 and 4. These histograms are based on all available 3 h observations during September–December for the 24-, 23- and 15-year periods at OWS P, N and V, respectively. About 96% of all possible reports are included in the case of the wind information, and a slightly small percentage for the Q_a values, because humidity measurements were missing more frequently. The mean values of u_* are equal to 0.42, 0.30 and 0.23 m s^{-1} at P, V and N, respectively, which is consistent with the distribution of westerly surface winds with latitude. OWS N tends to lie within the subtropical high pressure circulation with only moderate winds and few extreme values. By contrast, OWS P is affected by the passage of intense extratropical cyclones. Consequently, the u_*^3 values are distributed over a much larger range at OWS P than at N. The mean u_*^3 values are 0.13, 0.05 and 0.02 m^3 s^{-3} at P, V and N, respectively, which indicates a much different rate of turbulent kinetic energy production at the three locations.

The upward heat flux (Fig. 4) is also skewed relative to the mean values of 0.32, 0.55 and 0.43 ($\times 10^{-2}$) ly s^{-1} at P, V and N, respectively. A majority of the Q_a values lie below these mean values with a few large values accounting for the remaining flux. Although the larger variations in wind speed occur at P, the heat flux is larger at V. Monthly mean sea-air temperature differences at P are about 0.1°C in September and reach a maximum of 0.7°C in November. Corresponding mean vapor pressure differences are 1.9 and 2.3 mb in September and November. By contrast the mean sea-air temperature differences increase from 1.0°C in September to 2.4°C in December at V, with vapor pressure differences of about 8 mb throughout the cooling season. Because the air

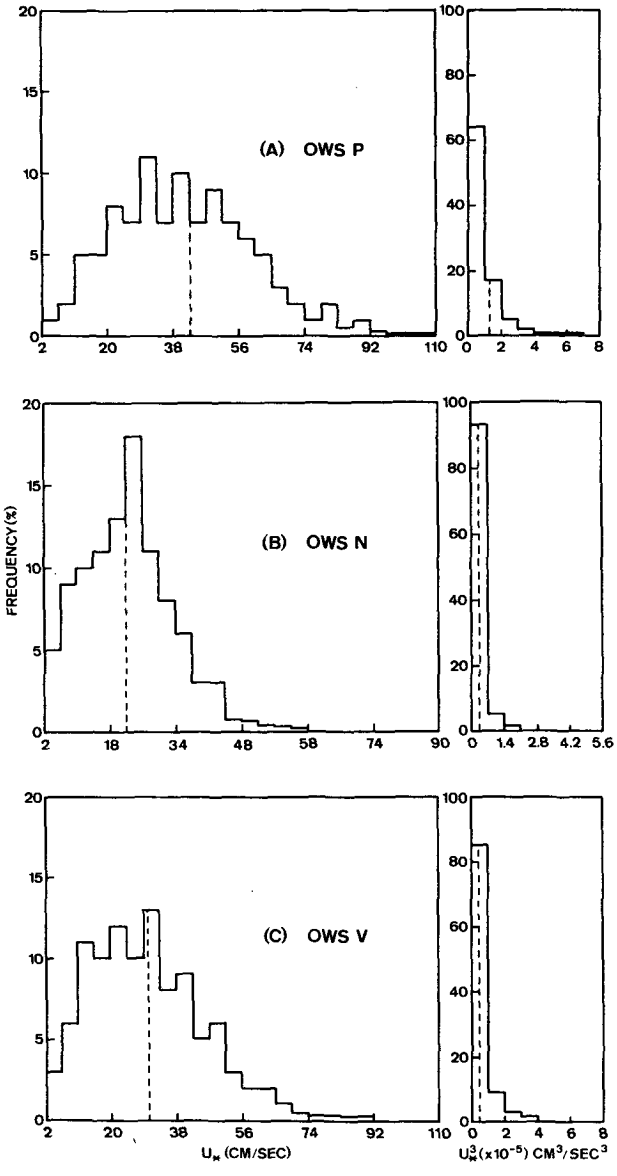

FIG. 3. Histograms of u_* and u_*^3 from the 3 h observations at OWS P, OWS N and OWS V. Vertical dashed lines represent the mean of the distributions; note the different abscissa scales.

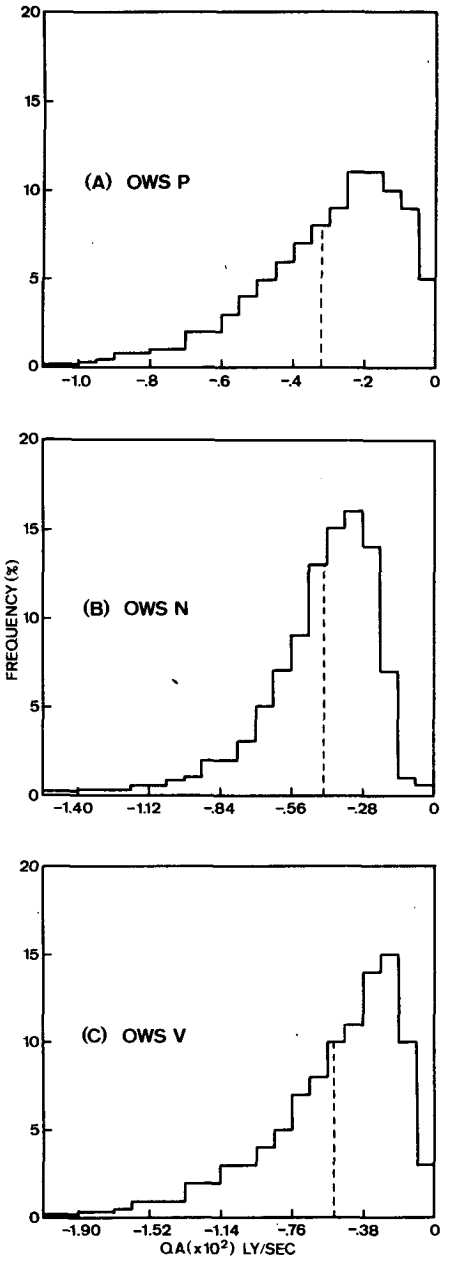

FIG. 4. As in Fig. 3 except for surface heat flux plus back radiation (Q_a).

parcels arriving at V may have had a relatively short overwater trajectory, the air-sea differences can be quite extreme for outbreaks of cold air behind extratropical cyclones (Manabe, 1958). At OWS P, the long overwater trajectories tend to result in near-equilibrium conditions, or even air temperatures exceeding ocean temperatures in the case of trajectories from the southwest. Thus, the air-sea differences in the western Pacific (V) are much larger and have greater variability than in the northeast Pacific.

The total mechanical and convective generation of turbulent kinetic energy is related to summation of the u_*^3 and Q_a distributions, respectively. To demonstrate the role of the large, but relatively rare, forcing events, the values were rank-ordered by magnitude and accumulated by months, seasons and as long-term means. One of the surprisingly consistent distributions is the percentage of the u_*^3 observations which account for particular percentages of the accumulated u_*^3. The curve for u_*^3 in Fig. 5 was found to apply within a few percent for individual monthly accumulations at all three stations during September through December. This u_*^3 curve may be represented by the function $FE^2 = 200\ PE - PE^2$, where FE is the cumulative percentage of observations and PE the cumulative percentage of the total u_*^3. That is, one consistently finds that about 87% of the smallest u_*^3 values must be summed to contribute only 50% of the accumulated u_*^3, which implies that the 13% consisting of the largest u_*^3 values contribute the remaining 50% of the total u_*^3. Although the total input of u_* and u_*^3 is quite different at the three stations and during the four months, the uniformity of the u_* and u_*^3 distributions in Fig. 5 is quite remarkable. This demonstrates the importance of a few large events in the mechanical production of turbulent kinetic energy, and is consistent with the characteristic rapid deepening in association with strong forcing events illustrated in Fig. 1B. One may infer that most of the turbulent kinetic energy generated by the small values of u_*^3 is expended to maintain the existing layer depth, or to oppose shallowing of the layer during heating periods. A burst of significantly larger values of u_*^3 is required to rapidly deepen the

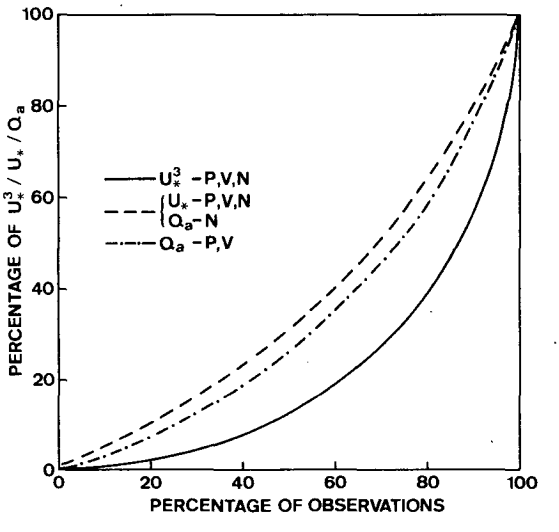

FIG. 5. Cumulative percentage of rank-ordered 3 h u_*, u_*^3 and Q_a values versus cumulative percentage of observations based on 24-, 15- and 23-year samples (September to December) at OWS P, V and N, respectively.

layer. It is also of interest to compare the cumulative heat flux distributions at the three stations. The Q_a distribution at OWS N follows the u_* distribution, which suggests that the variability in Q_a is associated with the wind speed rather than the air-sea temperature or vapor pressure differences. Much of the variability at OWS N then may be associated with surges in the wind flow, rather than frontal passages separating distinct air masses. The Q_a distributions for OWS P and V are also similar, and lie between the u_* and u_*^3 curves. About 50% of the accumulated Q_a is associated with about 74% of the smallest (ranked) Q_a fluxes. The remaining 26% consisting of the largest 3 h values of Q_a account for the other half of the accumulated Q_a. Simpson (1969) had earlier demonstrated that significant air-sea exchanges in mid-latitudes tend to be concentrated in synoptic-scale forcing events.

4. Characteristics of the synoptic event atmospheric forcing

In the previous section the 3 h observations of u_*^3 and Q_a were ranked according to magnitude, so that two similar values may have occurred in different years. In this section we examine the time series of u_*^3 and Q_a and define sustained periods of strong forcing as an "event". Although our information is limited to point measurements at the OWS locations, it is clear that these events may be associated with discrete synoptic-scale systems. The objectives of this analysis are to examine the principal characteristics of these synoptic events, to calculate the total energy exchange during these events, and to infer the oceanic response in terms of the sea-surface temperature change. The large data gaps in the bathythermograph record would not permit analysis of the mixed-layer changes during these events. However, the examples presented earlier, and the numerical simulations of Camp and Elsberry (1977), indicate that large changes in sea-surface temperature are normally accompanied by changes in mixed layer depth.

An "event" will be defined as the period of one day or more during which the atmospheric forcing was greater than the long-term mean for the corresponding day, as in Figs. 1 and 2. Separate analyses were made for events defined from the u_*^3 values (mechanical events) and from the Q_a values (cooling events). For example, in Fig. 2 there are five distinct periods during November 1959 in which the u_*^3 curve exceeded the long-term mean. The last period began in November and continued into December. Such an event would be credited to the month during which the largest fraction of the total energy flux occurred. One can also note that the maximum u_*^3 value during an event may just exceed the long-term mean value, or the peak value may be many times the mean value. Consequently it was useful to characterize the events in terms of the peak-to-mean ratio. As the duration of an event was defined as the total period for which the daily mean forcing exceeded the long-term mean, an interpolation in time was necessary to define the beginning and end of each event. With this definition of the initial and final time, the magnitude of the various fluxes and the simultaneously observed sea surface temperature change occurring during each event could be calculated and accumulated.

A summary of the characteristics of the mechanical (u_*^3) and cooling (Q_a) events with peak values exceeding the long-term mean is given in Table 1. A similar summary for events with the peak values exceeding the long-term mean by a factor of at least 1.5 is shown in Table 2. One of the most consistent results for both the seasonal totals, as in Table 1, and the monthly values (to be presented later) is the duration of the events. At each of the three stations about one-third of each period is affected by mechanical events, which implies that the average interval between events is about twice the length of the event. Cooling events tend to last somewhat longer because the large air-sea differences persist longer than the wind speed peak. If these events are important to the seasonal evolution, a significant fraction of the total energy flux should be associated with these events. One can see in Table 1 that between 68 and 77% of the total u_*^3 occurred during the roughly one-third of the time that mechanical events occurred. Conversely, only the remaining 23–32% of the total u_*^3 occurred during the two-thirds of the time that represent the intervals between events. As in the 3 h data, these statistics indicate the highly skewed nature of turbulent kinetic energy generation—but also that a significant fraction is associated with events having a synoptic time scale.

One can note from Table 1 that periods of mechan-

TABLE 1. Characteristic forcing and response during events with peak-to-mean ratios greater than 1.0. Values in parentheses are standard deviations about the mean.

Variable	Mechanical events			Cooling events		
	OWS P	OWS V	OWS N	OWS P	OWS V	OWS N
Duration (%)	36	33	36	46	41	43
u_*^3 (%)	70	68	77	69	59	69
Q_n (%)	56	61	97	97	90	119
ΔSST (%)	68	57	85	83	78	91
Number of events per month	5.1 (1.8)	4.4 (1.7)	3.8 (1.4)	4.4 (1.8)	4.3 (1.6)	3.8 (1.4)
Duration of events (days)	2.2 (1.7)	2.3 (1.7)	2.9 (2.4)	3.2 (3.1)	2.8 (2.2)	3.6 (3.4)
Peak-to-mean ratio	1.8 (.93)	1.9 (1.6)	2.1 (5.3)	1.4 (.39)	1.4 (.42)	1.3 (.35)

TABLE 2. Characteristic forcing and response during events with peak-to-mean ratios greater than 1.5. Values in parentheses are standard deviations about the mean.

Variable	Mechanical events			Cooling events		
	OWS P	OWS V	OWS N	OWS P	OWS V	OWS N
Duration (%)	22	20	22	19	17	15
u_*^3 (%)	48	44	55	34	30	33
Q_n (%)	35	37	71	45	46	63
ΔSST (%)	50	31	57	37	33	43
Number of events per month	2.4 (1.4)	2.4 (1.5)	1.9 (1.3)	1.4 (1.1)	1.4 (1.2)	.75 (.08)
Duration of events (days)	2.8 (1.8)	2.6 (1.6)	3.6 (2.7)	4.3 (3.5)	3.6 (2.0)	6.1 (4.7)
Peak-to-mean ratio	2.4 (1.0)	2.5 (2.0)	3.0 (7.4)	1.9 (.39)	1.9 (.38)	1.9 (.36)

ical events are also periods of significant net cooling ($Q_n = Q_a - Q_s$, where Q_s is the insolation). Only 56% of the net cooling at P occurs during mechanical events, whereas 97% of the net cooling at N is in association with mechanical events. Conversely one can note that longer lasting cooling events are associated with, but not identical to, significant fractions of total u_*^3 flux. Thus the definition of either a mechanical or a cooling event results in a similar illustration of the effect of events having a synoptic time scale. One can also see that the periods of upward heat flux (Q_a) greater than the long-term mean account for 90–119% of the net heat flux during the period September to December at the three stations. The values exceeding 100% may be explained by noting that the periods of upward heat flux associated with events can account for more than the monthly or seasonal flux which includes both upward and downward heat flux periods.

The thermal response during the events was estimated from the daily mean sea surface temperatures. If, as was the normal case, all the 3 h observations were available, the trend in the daily mean values was reasonably smooth. Long-term mean temperature decreases from the beginning of September to the end of December are about 7.0, 7.8 and 3.4°C at OWS P, V and N, respectively. The percentage of the seasonal sea surface temperature cooling (ΔSST) that occurred during mechanical events ranged from 57% at V to 85% at N. During the longer lasting cooling events the values ranged from 78 to 91% of the seasonal cooling. The importance of a correct specification of the forcing to predict the evolution of the mixed layer temperature during the relatively short, but intense synoptic events is evident from these percentages.

An indication of the frequency of cooling season forcing events with a peak value exceeding the long-term mean is also shown in Table 1. At OWS P there are typically 5.1 mechanical events lasting an average of 2.2 days during the September–December period. This is indicative of the frequent cyclonic and frontal system passages in this region. At OWS N there are 3.8 mechanical events with a longer duration (2.9 days), which is consistent with the identical 36% of the total time at both N and P. One may note again the close association of wind and cooling events at N in that there are also 3.8 cooling events. As noted earlier, the cooling events persist longer (3.6 days at N) than the mechanical events (2.9 days). Particularly at P there are fewer cooling events (but of longer duration) than mechanical events. Finally the average peak-to-mean ratio for the cooling events was about 2.0, which suggests that the sample included a number of relatively weak events, as well as the strong forcing events of the type illustrated in Figs. 1 and 2.

The characteristics and the associated thermal responses for events with peak-to-mean ratios of at least 1.5 are presented in Table 2. This selection process eliminated about half of the events that were included in Table 1. These stronger mechanical events are relatively rare occurrences as there are only 2.4 events per month at P and V and 1.9 per month at N. The periods with relatively small peak values also tended to be of short duration. Consequently the mean duration of the stronger mechanical events was greater at each station compared with the weaker events summarized in Table 1. One should note that about 50% of the total u_*^3 flux occurs during the 20–22% of the time associated with the stronger mechanical forcing events. Although the intervals between such events would average about four times the duration of the event, only 50% of the flux of u_*^3 occurs during these relatively weak forcing intervals. It should be noted again that the similarity of these percentages is quite remarkable in view of the large differences in the magnitudes of u_*^3 at the three locations. As in Table 1, the association between the mechanical events and the net heat flux is progressively larger from P to V to N. And as before, the thermal response in terms of the change in sea surface temperature ΔSST at P and N during the 22% of the time associated with the stronger wind events emphasizes the importance of these relatively rare events to the seasonal evolution. One can infer that an abnormal number of such forcing events during a month or a season could produce cold or warm anomalies of significant amplitude relative to the normal cooling during the period.

Definition of cooling events with the requirement that the peak-to-mean ratio be at least 1.5 (as in Table 2) decreased the number of these events by a factor at least 3 from the values in Table 1. The pattern of cooling with time tended to be less peaked than the u_*^3 distribution, but persisted for longer periods. Although the frequency dropped to 1.4 per

month at P and V and 0.75 at N, the duration of these stronger cooling events increased to 4.3, 3.6 and 6.1 days, respectively. The corresponding duration in percent of the time was 19, 17 and 15%. Nevertheless at least one-third of the net sea surface temperature change during the season was associated with these rare cooling events. Although these statistics do not explain the reasons why the strong events occur during some periods and not during others, it is clear that the presence or absence of just a few of these strong events may have a significant effect on the seasonal evolution.

The overall seasonal statistics in Table 1 were also divided into monthly periods for the 24, 15 and 23 years at P, V and N, respectively. The percent of time and the sea surface temperature change during the mechanical and cooling events with peak-to-mean ratio of at least 1.0 are summarized in Table 3. One of the most important points is the relative invariance at each station in the percentage of time that these events occur during September to December. Consequently, the seasonal percentage of time for these events in Table 1 is also reflected in each month, although the total forcing in each month varies. The larger variations in percent of time at V may be due to the smaller sample size at that station. The general character of the mechanical events being shorter in duration than the cooling events is maintained. However, the oceanic response to this essentially uniform frequency of events varies insignificantly through the season.

The largest percentage contribution to the oceanic response by the strong forcing events occurs during September at each station. September tends to be the transition month between the heating and cooling seasons, with the transition being progressively later in the equatorward stations. Mean sea-surface temperature changes during September are equal to −1.0°C at P and V and zero (standard deviation 0.9°C) at N. Thus the temperature decreases that occur during events in a month may exceed the observed decrease over the entire month. The implication is that the heat flux to the atmosphere exceeds the net insolation for the day only during periods of higher than average wind speed. As noted above, the largest sea surface temperature decrease will tend to occur when a warm and shallow mixed layer is present. Consequently, as the layer deepens during October and November the percent of the cooling during mechanical events tends to decrease as the role of the entrainment mixing at the base of the layer diminishes. As the extra cooling effect due to entrainment mixing associated with the mechanical production of turbulent kinetic energy accompanying synoptic events is reduced, the more uniform cooling due to surface fluxes during the intervals between events will play a more important role. At P the percentage of ΔSST associated with mechanical events increases during December, perhaps because the mean ΔSST change is only −1.2°C, compared with −2.8 and −2.0°C during October and November. In general, the cooling events have a similar effect to the mechanical events, but the percentages are larger. Inclusion of the longer periods with Q_a exceeding the long-term mean in these cooling events increases the dominance of these periods in the net cooling for the month over the intervals between events, which may be periods of downward heat flux.

TABLE 3. Percent of time and associated monthly sea surface temperature decrease during mechanical (u_*^3) and cooling (Q_a) events based on 24, 15 and 23 years at OWS P, V and N.

		September	October	November	December
			Mechanical events		
P	Time	35	36	36	37
	ΔSST	103	68	56	66
V	Time	28	35	34	35
	ΔSST	70	61	66	40
N	Time	35	37	37	37
	ΔSST	436	94	69	58
			Cooling events		
P	Time	44	49	49	46
	ΔSST	121	77	73	83
V	Time	36	40	45	37
	ΔSST	147	81	71	54
N	Time	46	43	41	42
	ΔSST	1838	103	78	61

5. Conclusions

The 3 h surface data from Ocean Weather Ships P, V and N have been examined to demonstrate the contribution of strong forcing events to oceanic cooling during September to December. The forcing is specified in terms of non-advective mixed layer dynamics, which Camp and Elsberry (1977) have shown to be capable of explaining a major fraction of the oceanic thermal structure modification during these periods of strong atmospheric forcing. Because bathythermographs were not taken as regularly or as frequently as the meteorological data, the oceanic thermal response was evaluated in terms of the changes in daily averaged sea surface temperature.

Although the total generation of turbulent kinetic energy by mechanical (u_*^3) or thermal (Q_a) forcing is quite different at the three locations, a very large percent of that total forcing occurs during a relatively small fraction of the time. By ranking the 3 h observations of u_*^3, it was demonstrated that about 13% of the largest u_*^3 values contribute 50% of the total u_*^3 at each station. The uniformity of the

cumulative u_* and u_*^3 distributions at the three stations is quite remarkable in view of the very different total inputs at the three stations. A similar distribution of cooling is found at OWS P and V, but this thermal forcing is less skewed than the u_*^3 input. The variability in Q_a at OWS N tends to follow the u_* distribution, which suggests that the variability of air-sea temperature differences is less important.

A synoptic forcing event was defined as the period during which the atmospheric forcing was greater than the long-term mean for the corresponding day. At OWS P there are typically 5.1 mechanical (u_*^3) events lasting an average of 2.2 days during the September–December period. An identical 36% of the time is associated with mechanical events at OWS N, even though the synoptic systems are different and the total forcing is much smaller than at P. The important point is that between 68 and 77% of the total u_*^3 occurred during the roughly one-third of the time associated with mechanical events. The events defined in terms of upward heat flux give a similar indication of the dominant role of synoptic-period systems in the mechanical and thermal forcing of the upper ocean. A significant fraction of the September–December sea surface temperature change occurs during these events. Consequently the presence or absence of a few of these strong forcing events during a month or season can have a significant effect on the seasonal evolution. Larger surface temperature changes occurred during strong events in September and early October, when the mixed layer was relatively warm and shallow. Thus, both the intensity and the timing of the synoptic period atmospheric forcing is needed to understand and predict the seasonal evolution of the upper ocean thermal structure.

Acknowledgments. The authors would like to thank Ms. Sharon Raney for her assistance in programming and execution of these calculations, which were done at the W. R. Church Computer Center. Professors R. L. Haney and D. F. Leipper made a number of helpful comments on the manuscript, which was typed in various versions by M. Marks and B. Swenson. This research was sponsored by Office of Naval Research (NR-083-275).

APPENDIX

Calculation of Atmospheric Forcing

Based on the recommendation of Gunter Seckel (personal communication), the solar insolation was estimated by

$$Q_s = (1 - a\alpha^b)(1 - 0.66C^3)Q_0,$$

where the clear-sky radiation (Q_0) is given by

$$Q_0 = A_0 + A_1 \cos\phi + B_1 \sin\phi + A_2 \cos 2\phi + B_2 \sin 2\phi$$

using harmonic coefficients of the values presented in the *Smithsonian Meteorological Tables* (List, 1958) with

$$\phi = \frac{2\pi}{365}(t - 21).$$

In these expressions t is the Julian day of the year, C the fractional total cloud cover, α the mid-day elevation angle of the sun, and the constants a and b were adapted from Tabata (1964). The net longwave radiation (Q_b) was calculated from a formula of Husby and Seckel (1975), i.e.,

$$Q_b = 1.14 \times 10^{-7}(T_s + 273.16)^4(0.39 - 0.05E_a^{1/2}) \times (1 - 0.6C^2),$$

where E_a is the saturated vapor pressure based on the reported dewpoint temperature.

Turbulent fluxes of latent heat (Q_e), sensible heat (Q_n) and momentum (τ_s) at the air-sea interface were calculated using the following bulk aerodynamic formulas:

$$\tau_s = \rho_a C_D \bar{u}_a^2, \qquad Q_h = C_D(T_s - T_a)\bar{u}_a,$$

$$Q_e = C_D(0.98E_s - E_a)\bar{u}_a, \qquad Q_a \equiv Q_b + Q_e + Q_h,$$

where $\bar{u}_a$ is the mean wind speed (m s^{-1}), T_a the air temperature (°C), E_s the saturated vapor pressure of the marine air directly in contact with the sea surface (0.98 corrects for salt effects), and C_D the nondimensional drag coefficient. A constant drag coefficient (1.3×10^{-3}) was used in all computations.

REFERENCES

Camp, N. T., 1976: The role of strong atmospheric forcing events in the modification of the upper ocean thermal structure during the cooling season. Ph.D. dissertation, Naval Postgraduate School, Monterey, 175 pp.

——, and R. L. Elsberry, 1977: Oceanic thermal response to strong atmospheric forcing. II. The role of one-dimensional processes. *J. Phys. Oceanogr.*, **8**, 215–224.

Husby, D. M., and G. R. Seckel, 1975: Large-scale air-sea interactions at Ocean Weather Station V, 1951–1971. NOAA Tech. Rep. NMFS SSRF-696, 44 pp.

List, R. J., 1958: *Smithsonian Meteorological Tables*. Smithsonian Institution, 527 pp.

Manabe, S., 1958: On the modification of air mass over the Japan Sea when the outburst of cold air predominates. *J. Meteor. Soc. Japan*, Ser. II, **35**, 311–326.

Simpson, J., 1969: On some aspects of sea-air interaction in middle latitudes. *Deep-Sea Res.*, Suppl., **16**, 233–261.

Tabata, S., 1964: A study of the main physical factors governing the oceanographic conditions of station P in the northeast Pacific Ocean. D.Sc. thesis, University of Tokyo, 264 pp.